Visual assessment of ^{18}F-FDG metabolic spatial distribution improves the differential diagnosis of indeterminate pulmonary nodules and masses with high FDG uptake

Jie Lin
Wenzhou Medical University First Affiliated Hospital
Ling Wang
Wenzhou Medical University First Affiliated Hospital
Xiaowei Ji
Wenzhou Medical University First Affiliated Hospital
Xiangwu Zheng
Wenzhou Medical university First Affiliated Hospital
Kun Tang (kuntang007@163.com)
The First Affiliated Hospital of Wenzhou Medical University

Original research

Keywords: Fluorodeoxyglucose F18, Positron emission tomography, Metabolic, Lung cancer

Posted Date: March 20th, 2020

DOI: https://doi.org/10.21203/rs.3.rs-18135/v1

Abstract

Purpose The aim of this study was to evaluate the value of visual analysis of 18 F-fluorodeoxyglucose (18 F-FDG) metabolic spatial distribution (V-FMSD) in diagnosis of indeterminate pulmonary nodules and masses with high 18 F-FDG uptake.

Methods A total of 301 patients with indeterminate pulmonary nodules or masses who undergone 18 F-FDG positron emission tomography/computed tomography (PET/ CT) imaging were studied retrospectively. The characteristics of 18 F-FDG metabolic spatial distribution (FMSD) of proximal and distal regions of the lesion were visually analyzed using a 5-point scoring system. The sensitivity, specificity, accuracy and area under receiver operating characteristic curve (AUC) were compared between V-FMSD and conventional PET/CT methods for diagnosis of hypermetabolic indeterminate pulmonary nodules and masses.

Results The V-FMSD results showed that 180 (92.8%) malignant lesions' scores were ≥ 3 and 78 (72.9%) benign lesions' scores were ≤ 2. It indicated that the FMSD in the proximal region of malignant lesions was significantly higher than that of the distal region, and the FMSD in the proximal region of benign lesions was significantly lower than that of the distal region. The specificity of V-FMSD was 72.9%, which was obviously higher than the maximum standard uptake value (SUVmax) (0%, $P < 0.001$) and retention index (RI) (26.2%, $P < 0.001$). The AUC of V-FMSD was 0.886, which was significantly larger than SUVmax (0.626, $P < 0.001$), RI (0.670, $P < 0.001$) and PET/CT (0.788, $P < 0.05$).

Conclusions The characteristics of FMSD between pulmonary benign and malignant lesions are different. V-FMSD can be taken as a novel auxiliary marker to improve the diagnostic performance for hypermetabolic indeterminate pulmonary nodules and masses.

Introduction

The incidence of lung cancer is continuous rising because of the improvement in healthcare and population aging in the world. It has become the leading cause of cancer death in United States.[1] Early detection strategies and surgical resection are key to reduce the mortality of lung cancer.[2]

Positron emission tomography / computed tomography (PET/CT) is a noninvasive imaging technique which is widely used in diagnosis of pulmonary nodules.[3, 4] The maximum standard uptake value (SUVmax) is a main semiquantitative method for PET to identify the metabolic activity of lesion. A SUVmax of 2.5 is usually used as the critical value to differentiate malignant from benign pulmonary lesions. However, ^{18}F-fluorodeoxyglucose (^{18}F-FDG) is not a tumor specific agent, thus intense FDG uptake can be observed in a significant percentage of benign pulmonary lesions, such as inflammatory pseudotumor, cryptococcosis, tuberculosis, and so on. [5, 6] Therefore, high false positive rates in diagnosis of pulmonary lesions caused by SUV were reported in previous studies.[7, 8] Especially when the morphological characteristics of benign and malignant lesions are atypical, the false positive rate is

higher. Then, unnecessary invasive surgery to the lung and associated morbidity were correspondingly increased because of high false positive results.[9]

Therefore, a new alternative way derived from PET/CT is urgently needed to compensate for the high false positive rate caused by SUV method. Since cancer cells intent to invade blood vessels[10], it can be speculated that cell metabolic activity will be higher in the proximal part of malignant tumor than that of the distal part. Our previous findings have confirmed that the relative activity distribution (RAD) of ^{18}F-FDG in malignant and benign solitary pulmonary nodules (SPNs) was obviously different. Furthermore, use of the characterization of SPNs with ^{18}F-FDG RAD seems to be much more specific than conventional SUV diagnostic method in differentiating malignant and benign SPNs.[11] However, the previous study only analyzed local metabolic distribution on small pulmonary nodules, and the data need to be obtained by complex diameter measurement and calculation. Therefore, the clinical feasibility of ^{18}F-FDG metabolic spatial distribution (FMSD) in differentiating pulmonary nodules needs a wider range of samples and further simplification.

The aim of present study thus was to evaluate whether visual assessment of ^{18}F-FDG metabolic spatial distribution (V-FMSD), an easy-to-operate method, can improve the value in differential diagnosis of high metabolic pulmonary nodules and masses.

Materials And Methods

Patients

This retrospective study included 301 consecutive subjects (186 men and 115 women; mean age 61.6 ± 11.2 years; range 21 - 89 years) who underwent FDG PET/computed tomography (CT) for suspect malignant pulmonary nodules or masses between January 1, 2015 and April 26, 2017. The exclusion criteria used in present study was listed as follows:

1. ^{18}F-FDG SUVmax of lesions < 2.5;
2. With typical benign signs (central laminated or diffuse calcification, popcorn pattern of calcification) or malignant signs (has any three of following signs: densely spiculated margin, vacuole sign, air bronchogram, vessel convergence, pleural indentation, lesion with cavitations and wall thickness > 16 mm) detected by chest CT;
3. Metastatic lesions or with evidence of metastasis;
4. With multiple hypermetabolic nodules or masses in both lungs;
5. Received lung biopsy or neoadjuvant chemoradiotherapy prior to PET/CT examination;
6. With previous history of other cancer.
7. With obvious motion or breathing artifact.

The patients were performed fibrobronchoscopy, percutaneous biopsy, resection by thoracotomy, video-assisted thoracoscope surgery or follow-up after PET/CT examination. All malignant lesions were finally confirmed by pathology, and a definitive diagnosis of benign lesion was based on pathological analysis or at least 2 years of follow-up by chest CT. The study was approved by the institutional review board, and written informed consents were obtained from all participants.

PET/CT Acquisition

Patients fasted for at least 6 hours and serum glucose levels were < 110 mg/dl prior to intravenous injection of ^{18}F-FDG (3.7 MBq/kg). Approximately 60 min later, images were acquired by a hybrid PET/CT scanner (GEMINI TF 64, Philips, Netherlands). A whole-body unenhanced CT scan was performed from the skull base to the middle of thigh, with the following parameters: tube voltage of 120 kV, tube current of 249 mA, detector collimation of 64 × 0.625 mm, pitch of 0.829, a tube rotation speed of 0.5 s, section thickness of 5.0 mm, and reconstruction thickness of 2.5 mm. After the CT scan, PET emission scans were acquired in a three-dimension mode with field of view (FOV) of 576 mm, matrix of 144 × 144, slice thickness and interval of 5.0 mm. The dual time point scans were performed for pulmonary lesions 120 min after the injection. PET images were reconstructed using the ordered subset expectation maximization (OSEM) method (33 subsets per iteration). All collected data was transferred into Philips Extend Brilliance Workstation (EBW) 3.0 to reconstruct PET, CT and PET / CT fusion images.

Image Analysis

Data measurement was independently performed by one experienced nuclear medicine physician. The SUVmax values of early and delay scans were quantified for each lesion. The retention index (RI) was calculated according to the following formula:

$$RI = \frac{100\% * (Dual\ time\ point\ SUVmax - Early\ SUV\max)}{\text{Early SUVmax}}$$

For SUV assessment, the findings were considered as positive when SUVmax ≥ 2.5, and for delay PET scan, RI > 0 was defined as positive.

The combined PET/CT assessments were performed by two radiologists with over 30 years of experience in radiologic diagnosis who were ignored the characteristics of ^{18}F-FDG spatial distribution of lesions. First, the definitely positive findings were considered when ^{18}F-FDG uptake of lesion were significantly higher than that of the mediastinal blood pool. Second, the remain lesions were classified as probably positive or probably negative ones according to the morphological characteristics on simultaneous low-dose CT images. Finally, definitely or possibly positive lesions were recorded as positive, and possibly negative lesions were recorded as negative.

The V-FMSD were analyzed by two nuclear medicine physicians with 10 years of experience in PET/CT diagnosis who were blinded to the information of CT images and the final diagnoses of the patients. The

proximal region of lesion was defined as the area near the ipsilateral hilar, and the area far from the ipsilateral hilar was defined as the distal region.[12] A 5-point scoring system was used to interpret the characteristics of FMSD, which represent the likelihood of the lesion being benign or malignant (Table 1). When the characteristics of FMSD in lesions are not obvious, the metabolic threshold can be manually adjusted on transverse PET images to assist the interpretation. When the interpretation scores are inconsistent between two readers, a consensus will be made by discussion. Finally, a score ≤ 2 was recorded as negative, while a score ≥ 3 was recorded as positive.

Table 1
The 5-point scoring system for interpretation of the characteristics of FMSD

Scores	FDG uptake		Interpretation
	Proximal region	Distal region	
1	Significantly lower	Significantly higher	Definitely benign
2	Slightly lower	Slightly higher	Probably benign
3	Roughly homogeneous	Roughly homogeneous	indeterminate
4	Slightly higher	Slightly lower	Probably malignant
5	Significantly higher	Significantly lower	Definitely malignant

Statistical Analysis

Statistical analyses were performed with SPSS software, version 23.0 (SPSS, Chicago, USA). The Mann–Whitney U-test was used to evaluate the continuous variables between malignant and benign lesions, and the results were described as means ± standard deviations. The chi-squared test was performed to analyze the categorical data, and the results were presented as frequency and percentage. Receivers operating characteristic (ROC) was used to assess the performance of SUVmax, RI, combined PET/CT assessment and V-FMSD for distinguishing malignant and benign lesions. The corresponding sensitivity, specificity, accuracy, positive predictive value (PPV) and negative predictive value (NPV) for each diagnostic method were calculated respectively. The McNemar test was used to compare the sensitivity, specificity and accuracy of V-FMSD with those of the other methods. The intra-observer variability in visual scores was determined by use of the Cohen's kappa coefficient (κ). A P-value of < 0.05 was considered statistically significant.

Results

General Characteristic of Subjects

Among all 301 nodules and masses, 194 (64.5%) were malignant, and 107 (35.5%) were benign. The average maximum diameter of lesions was 27.7 ± 13.2 mm (range 8–63 mm). The malignant lesions were pathologically confirmed as adenocarcinoma (129, 66.5%), squamous cell carcinoma (41, 21.1%), adenosquamous carcinoma (13, 6.7%), sarcomatoid carcinoma (3, 1.6%), small cell carcinoma (4, 2.1%)

and neuroendocrine carcinoma (4, 2.1%). The benign lesions confirmed by pathology or follow-up included tuberculosis (45, 42.1%), inflammatory pseudotumor (3, 2.8%), interstitial pneumonia (2, 1.9%), focal organizing pneumonia (8, 7.5%), angiofollicular hyperplasia (1, 0.9%), chronic inflammation (12, 11.2%), cryptococcal disease (18, 16.8%), sclerotic hemangioma (9, 8.4%), silicotic nodule (1, 0.9%), granulomatous inflammation (6, 5.6%) and fungus infection (2, 1.9%). The general characteristics of benign and malignant lesions were shown in Table 2. Compared with benign lesions, the malignant tumors presented significantly higher values in lesion size, SUVmax, delay SUVmax and RI.

Table 2
General Characteristics of Subjects

Characteristics	Overall (n = 301)	Benign (n = 107)	Malignant (n = 194)	P value
Age, years	61.6 ± 11.2	57.6 ± 12.6	63.9 ± 9.6	< 0.001
Sex				0.014
Male, n (%)	186 (61.8)	76 (71.0)	110 (56.7)	
Female, n (%)	115 (38.2)	31 (29.0)	84 (43.3)	
Tumor site				0.128
RUL, n (%)	99 (32.9)	42 (39.3)	57 (29.4)	
RML, n (%)	20 (6.6)	6 (5.6)	14 (7.2)	
RLL, n (%)	75 (24.9)	26 (24.3)	49 (25.3)	
LUL, n (%)	67 (22.3)	16 (15.0)	51 (26.3)	
LLL, n (%)	40 (13.3)	17 (15.9)	23 (11.9)	
Tumor size, mm	27.7 ± 13.2	24.2 ± 13.4	29.6 ± 12.8	0.001
FBG, mg/dl	5.6 ± 1.2	5.6 ± 1.5	5.5 ± 1.1	0.574
SUVmax	6.7 ± 3.9	5.7 ± 3.4	7.3 ± 4.0	< 0.001
Delay SUVmax	7.9 ± 5.0	6.0 ± 3.6	8.6 ± 5.3	0.001
RI (%)	26.1 ± 21.8	16.8 ± 21.6	29.8 ± 20.9	0.001

The V-FMSD Scoring Results

The visual scoring results of FMSD in benign and malignant lesions were demonstrated in Table 3. There were 180 (92.8%) malignant lesions with a score ≥ 3, which indicated that FDG metabolic distribution in proximal region of malignant lesion was significantly higher than that of distal region (Fig. 1). There were 78 (72.9%) benign lesions with a score ≤ 2, which indicated that FDG metabolic distribution in proximal region of benign lesion was significantly lower than that of distal region (Fig. 2). The visual scoring

results of FMSD in different size groups were demonstrated in Table 4. The intra-observer variability in visual scores by two observers was showed in Table 5. The Cohen's kappa coefficient showed a good agreement between the two observers' visual scores with a kappa value of 0.635.

Table 3
The scoring results of V-FMSD in benign and malignant lesions

Scoring	1	2	3	4	5	Overall
Benign lesions, n	15	63	20	7	2	107
Malignant lesions, n	0	14	51	92	37	194

Table 4
The scoring results of V-FMSD in different size groups

Size groups	Scoring					Overall
	1	2	3	4	5	
< 10 mm, n	0	1	1	1	0	3
10 ~ 19 mm, n	2	36	21	16	5	80
20 ~ 29 mm, n	7	20	29	36	14	106
30 ~ 49 mm, n	5	16	15	38	15	89
≥ 50 mm, n	1	4	5	8	5	23

Table 5
The assessment of intra-observer variability in visual scores

Observer 2	Observer 1					Overall
	1	2	3	4	5	
1	14	5	1	0	0	20
2	5	53	14	4	0	76
3	0	3	44	10	1	58
4	0	3	12	62	8	85
5	0	1	6	12	43	62
Overall	14	65	81	97	44	301
Kappa value 0.635						

The Diagnostic Performance of Different Methods

The performance of V-FMSD for distinguishing malignant and benign lesions was showed in Table 6. When the method of V-FMSD scoring ≥ 3 was used as the diagnostic criteria, the sensitivity, specificity, accuracy, PPV and NPV of the diagnosis were 92.8%, 72.9%, 85.7%, 86.1%, and 89.2%, respectively. The diagnostic performance of V-FMSD in different size groups showed no significance in distinguishing malignant and benign lesions (P all > 0.05). Compared with conventional PET/CT methods, although the sensitivity of V-FMSD was not significantly difference from the other three methods (P all > 0.05), the specificity (72.9%) was significantly higher than SUVmax (0%, P < 0.001) and RI (26.2%, P < 0.001) (Table 7).

The ROC curves plotted by different methods for diagnosis of malignant and benign lesions were drawn as shown in Fig. 3. The area under the ROC curves (AUCs) of SUVmax, RI, combined PET/CT assessment and V-FMSD were 0.626, 0.670, 0.788 and 0.886 respectively. The AUC of V-FMSD was significantly larger than SUVmax, RI and combined PET/CT (P all < 0.05) (Table 8).

Table 6
The performance of V-FMSD for distinguishing benign and malignant lesions

Groups	FN	FP	TP	TN	Sensitivity	Specificity	Accuracy	PPV	NPV
Overall, n = 301	14	29	180	78	92.8	72.9	85.7	86.1	89.2
< 10 mm, n = 3	0	1	1	1	/	/	/	/	/
10 ~ 19 mm, n = 80	3	11	31	35	91.2	76.1	82.5	73.8	92.1
20 ~ 29 mm, n = 106	5	7	72	22	93.5	75.9	88.7	91.1	81.5
30 ~ 49 mm, n = 89	5	8	60	16	92.3	66.7	85.4	88.2	69.6
≥ 50 mm, n = 23	1	2	16	4	94.1	66.6	87.0	88.9	80.0

Table 7

Comparison of diagnostic value among different methods

	FN	FP	TP	TN	Sensitivity	Specificity	Accuracy	PPV	NPV
SUVmax ≥ 2.5	0	107	194	0	100	0	64.5	64.5	0
Dual time point RI (%) > 0	9	79	185	28	95.3	26.2	70.8	71.2	78.0
Visual PET/CT assessment	8	41	186	66	95.9	61.7	83.7	81.9	83.7
V-FMSD Scoring ≥ 3	14	29	180	78	92.8	72.9*	85.7	86.1	89.2
* Significant difference (P < 0.001) between specificity of visual score and specificity of SUVmax and dual time point RI.									

Table 8

Comparison of AUCs among different methods

Variable(s)	Area	Std. Error	Significance	95% CI		Z value	P value
				Lower	Lower		
V-FMSD	.886	.021	.000	.845	.928		
SUVmax	.626	.033	.000	.561	.691	6.646[a]	< 0.05
RI	.670	.033	.000	.605	.735	5.521[b]	< 0.05
PET/CT	.788	.031	.000	.727	.848	2.615[c]	< 0.05
Z value = a. V-FMSD vs SUVmax; b. V-FMSD vs RI; c. V-FMSD vs PET/CT.							

Discussion

The present study firstly evaluated the performance of V-FMSD for distinguishing pulmonary malignant and benign lesions. The results indicated that FDG uptake in proximal region of malignant lesion was significantly higher than that of distal region, and the FMSD of benign lesion was opposite to that of malignant lesion. Furthermore, the characteristic of FMSD presented higher diagnostic efficiency, especially specificity, in diagnosis of pulmonary hypermetabolic lesions than other conventional PET/CT methods. Therefore, it should be considered as an additionally valuable investigation in processing those indeterminate pulmonary lesions.

^{18}F-FDG PET/CT is a well-established imaging modality in the diagnosis of most patients with suspected lung cancers. However, the overlap of SUVmax between benign and malignant pulmonary lesions limits

its diagnostic value. As reported by previous literatures, the specificity of PET for diagnosis of malignant pulmonary nodules varied from 13–89% across different studies.[13–17] It has been found that 73% of the benign non-neoplastic lesions with increased ^{18}F-FDG uptake were inflammatory lesions.[18] The mechanism of ^{18}F-FDG uptake in inflammatory and oncological diseases is similar and is mediated by glucose transporters Glut1-5[19] representing the levels of cellular glucose metabolism. In active inflammation and granulomatous diseases, such as tuberculosis and sarcoidosis, increased ^{18}F-FDG accumulation is showed in cells due to the expression of glucose transporters, especially Glut 1 in activated leucocytes, macrophages and T-lymphocytes.[20–22]

Since the prevalence of tuberculosis in China is higher than Western countries, the accuracy of ^{18}F-FDG PET/CT in identification of pulmonary abnormalities may be decreased. In present study, nearly half of (42.1%) benign lesions were tuberculosis, and the average SUVmax of those tubercular lesions was 6.7. Because all the cases included in this study had hypermetabolic lesions with SUVmax greater than 2.5, when SUVmax 2.5 was used as the cut-off value to diagnose lung cancer, the number of false positive cases was 107, the specificity and accuracy were 0% and 64.5%, respectively. It showed that the value of SUVmax in the diagnosis of hypermetabolic lung nodules and masses was very limited. Compared with SUVmax, PET/CT combines lesion morphology and metabolic information. However, for those hypermetabolic pulmonary nodules and masses with atypical CT morphology, the diagnostic basis is more dependent on the metabolic information of the lesion. In this study, the number of false positive cases of PET/CT combined analysis was 41, of which tuberculosis and cryptococcal bacteria accounted for a large proportion. Therefore, in order to further improve the diagnostic efficacy of high metabolic nodules and masses, it is necessary to explore a new auxiliary analysis method.

Our previous study has confirmed the difference of the relative activity distribution of ^{18}F-FDG between malignant and benign SPNs.[11] To further simplify the evaluation, the present study used the hilar as a reference to divide the lesions into proximal and distal regions, and visually interpreted the spatial distribution of ^{18}F-FDG uptake in the two regions of benign and malignant lesions. The results of this study showed that in the malignant lesions, the ^{18}F-FDG uptake in the proximal region was significantly higher than that of the distal region. In the benign lesions, the spatial distribution of ^{18}F-FDG was opposite to that of the malignant lesions, that is, the ^{18}F-FDG uptake in the proximal region is lower than that in the distal region. For the pathological mechanisms of the differences in metabolic spatial heterogeneity between benign and malignant lesions, one of the possible reasons may be related to angiogenesis and its distribution. Recently, increasing researches indicated that angiogenesis played an important role in tumor formation, growth, metastasis and recurrence.[23, 24] Abnormal tumor vasculature may lead to altered perfusion, which is believed to be a major extrinsic driver of metabolism through effects on oxygen and substrate delivery.[25] In addition, the main blood supply of lung cancer is bronchial artery, while the inflammation is more likely to stimulate extrapulmonary circulation artery to participate in blood supply. Therefore, the blood supply in proximal region of lung cancer is more abundant and the same phenomenon can be observed in distal region of lung inflammation. However, the metabolic

distribution in lesion is influenced by many factors, and other reasons may include tumor microenvironment, genetic heterogeneity, immune, and so on.[26–28]

The main advantage of this study is its simple operability. V-FMDS is simple and easy to operate in clinic. Furthermore, this simple visual analysis can achieve high diagnostic performance. Although the sensitivity of V-FMDS was similar with PET/CT conventional markers, the specificity of this new method was significantly higher than SUVmax and RI (P all < 0.001). In addition, the diameter of the lesions selected in this study ranged from 8–63 mm (27.7 ± 13.2 mm), which can more fully reflect the metabolic spatial heterogeneity in pulmonary lesions than our previous studies.[11] However, the visual difference of metabolic distribution in small nodules was not obvious due to its small volume, especially for those nodules less than 10 mm in size. However, the diagnostic performance of V-FMSD in different size groups (larger than 10 mm) showed no significance in distinguishing malignant and benign lesions. Compared with previous published literatures, our results including PET/CT conventional markers still showed relatively lower sensitivity and specificity. [3, 29, 30] The major reason might be the high proportion of benign hypermetabolic lesions included in this study. However, this novel visual assessment still can improve diagnostic performance when the CT morphology is atypical. Therefore, V-FMDS can be considered as a new routine auxiliary diagnostic method for the diagnosis of indeterminate pulmonary nodules and masses with high ^{18}F-FDG uptake.

The main limitation of this study is that visual analysis is a subjective empirical judgment, so there is subjective bias. In the present study, the Kappa value for evaluation of intra-observer variability was 0.635, which suggested that the consistency was good. In clinical practice, multiple observation exercises and comparative analysis of FMDS by adjusting the SUV threshold can be used to improve the repeatability of the assessment. In patient selection, we only included those pulmonary nodules and masses with avid ^{18}F-FDG uptake, so there was selective bias. In addition, this study did not explore related molecular mechanisms, but in our pre-experiment we found that the number of CD31 and epidermal growth factor receptor (EGFR) expression are different between proximal and distal regions in lung benign and malignant lesions, suggesting that the difference of FMDS may be correlated with tumor angiogenesis and its distribution. Therefore, the possible related mechanisms would be explored in further study.

Conclusions

The characteristics of FMSD between pulmonary benign and malignant lesions are different. FDG uptake in proximal region of malignant lesion was significantly higher than that of distal region, and the FMSD of benign lesion was opposite to that of malignant lesion. V-FMSD is a simple and easy to operate method, therefore, it can be taken as a novel auxiliary marker in clinic to improve the diagnostic performance for those indeterminate pulmonary nodules and masses with avid ^{18}F-FDG uptake.

Abbreviations

^{18}F-FDG Fluorine-18-fludeoxyglucose

PET/CT Positron emission tomography/computed tomography

SUV The standardized uptake value

SUVmax The maximum standardized uptake value

FMSD ^{18}F-FDG metabolic spatial distribution

V-FMSD Visual assessment of ^{18}F-FDG metabolic spatial distribution

RI Retention index

ROC Receivers operating characteristic

Declarations

Acknowledgements

The authors are grateful to Xiang-wu Zheng and Kun Tang for their help in visual assessment of ^{18}F-FDG metabolic spatial distribution.

Availability of data and materials

The datasets used and/or analyzed during the current study are available from the corresponding author on reasonable request.

Authors' contributions

Jie Lin and Ling Wang was involved in PET analysis and manuscript preparation. Xiang-wu Zheng and Kun Tang was involved in study design, image analysis. Ling Wang and Xiao-wei Ji were involved in data collecting. All authors read and approved the final manuscript.

Ethics approval and consent to participate

All procedures performed in studies involving human participants were in accordance with the ethical standards of the institutional and/or national research committee and with the 1964 Declaration of Helsinki and its later amendments or comparable ethical standards. For this type of study, formal consent is not required. Informed consent was obtained from all individual participants included in the study.

Consent for publication

Not applicable

Competing interests

Not applicable

Funding

This work was supported by Public Projects of Zhejiang Province (No. LGF19H180012).

References

1. Siegel R, Naishadham D, Jemal A. Cancer statistics, 2012. CA Cancer J Clin. 2012;62:10-29. doi:10.3322/caac.20138.
2. Patz EF, Jr., Rossi S, Harpole DH, Jr., Herndon JE, Goodman PC. Correlation of tumor size and survival in patients with stage IA non-small cell lung cancer. Chest. 2000;117:1568-71.
3. Garcia-Velloso MJ, Bastarrika G, de-Torres JP, Lozano MD, Sanchez-Salcedo P, Sancho L, et al. Assessment of indeterminate pulmonary nodules detected in lung cancer screening: Diagnostic accuracy of FDG PET/CT. Lung Cancer. 2016;97:81-6.
4. Zhang Y, Ni J, Wei K, Tian J, Sun S. CT, MRI, and F-18 FDG PET for the detection of non-small-cell lung cancer (NSCLC): A protocol for a network meta-analysis of diagnostic test accuracy. Medicine (Baltimore). 2018;97:e12387. doi:10.1097/MD.0000000000012387.
5. Sanchez-Montalva A, Barios M, Salvador F, Villar A, Tortola T, Molina-Morant D, et al. Usefulness of FDG PET/CT in the management of tuberculosis. PLoS One. 2019;14:e0221516. doi:10.1371/journal.pone.0221516.
6. Chang JM, Lee HJ, Goo JM, Lee HY, Lee JJ, Chung JK, et al. False positive and false negative FDG-PET scans in various thoracic diseases. Korean journal of radiology. 2006;7:57-69. doi:10.3348/kjr.2006.7.1.57.
7. Feng M, Yang X, Ma Q, He Y. Retrospective analysis for the false positive diagnosis of PET-CT scan in lung cancer patients. Medicine (Baltimore). 2017;96:e7415. doi:10.1097/MD.0000000000007415.
8. Maiga AW, Deppen SA, Mercaldo SF, Blume JD, Montgomery C, Vaszar LT, et al. Assessment of Fluorodeoxyglucose F18-Labeled Positron Emission Tomography for Diagnosis of High-Risk Lung Nodules. JAMA Surg. 2018;153:329-34. doi:10.1001/jamasurg.2017.4495.
9. Grogan EL, Deppen SA, Ballman KV, Andrade GM, Verdial FC, Aldrich MC, et al. Accuracy of fluorodeoxyglucose-positron emission tomography within the clinical practice of the American College of Surgeons Oncology Group Z4031 trial to diagnose clinical stage I non-small cell lung cancer. Ann Thorac Surg. 2014;97:1142-8. doi:10.1016/j.athoracsur.2013.12.043.
10. Wu PH, Giri A, Sun SX, Wirtz D. Three-dimensional cell migration does not follow a random walk. Proc Natl Acad Sci U S A. 2014;111:3949-54. doi:10.1073/pnas.1318967111.
11. Zhao L, Tong L, Lin J, Tang K, Zheng S, Li W, et al. Characterization of solitary pulmonary nodules with 18F-FDG PET/CT relative activity distribution analysis. Eur Radiol. 2015;25:1837-44. doi:10.1007/s00330-015-3592-8.

12. Wu L, Cao G, Zhao L, Tang K, Lin J, Miao S, et al. Spectral CT Analysis of Solitary Pulmonary Nodules for Differentiating Malignancy from Benignancy: The Value of Iodine Concentration Spatial Distribution Difference. Biomed Res Int. 2018;2018:4830659. doi:10.1155/2018/4830659.
13. van Gomez Lopez O, Garcia Vicente AM, Honguero Martinez AF, Jimenez Londono GA, Vega Caicedo CH, Leon Atance P, et al. (18)F-FDG-PET/CT in the assessment of pulmonary solitary nodules: comparison of different analysis methods and risk variables in the prediction of malignancy. Transl Lung Cancer Res. 2015;4:228-35. doi:10.3978/j.issn.2218-6751.2015.05.07.
14. Li Y, Su M, Li F, Kuang A, Tian R. The value of (1)(8)F-FDG-PET/CT in the differential diagnosis of solitary pulmonary nodules in areas with a high incidence of tuberculosis. Ann Nucl Med. 2011;25:804-11. doi:10.1007/s12149-011-0530-y.
15. Hashimoto Y, Tsujikawa T, Kondo C, Maki M, Momose M, Nagai A, et al. Accuracy of PET for diagnosis of solid pulmonary lesions with 18F-FDG uptake below the standardized uptake value of 2.5. J Nucl Med. 2006;47:426-31.
16. Taralli S, Scolozzi V, Foti M, Ricciardi S, Forcione AR, Cardillo G, et al. (18)F-FDG PET/CT diagnostic performance in solitary and multiple pulmonary nodules detected in patients with previous cancer history: reports of 182 nodules. Eur J Nucl Med Mol Imaging. 2019;46:429-36. doi:10.1007/s00259-018-4226-6.
17. Matthies A, Hickeson M, Cuchiara A, Alavi A. Dual time point 18F-FDG PET for the evaluation of pulmonary nodules. J Nucl Med. 2002;43:871-5.
18. Metser U, Even-Sapir E. Increased (18)F-fluorodeoxyglucose uptake in benign, nonphysiologic lesions found on whole-body positron emission tomography/computed tomography (PET/CT): accumulated data from four years of experience with PET/CT. Semin Nucl Med. 2007;37:206-22. doi:10.1053/j.semnuclmed.2007.01.001.
19. Brown RS, Leung JY, Kison PV, Zasadny KR, Flint A, Wahl RL. Glucose transporters and FDG uptake in untreated primary human non-small cell lung cancer. J Nucl Med. 1999;40:556-65.
20. Huber H, Hodolic M, Stelzmuller I, Wunn R, Hatzl M, Fellner F, et al. Malignant disease as an incidental finding at F-18-FDG-PET/CT scanning in patients with granulomatous lung disease. Nucl Med Commun. 2015;36:430-7. doi:10.1097/Mnm.0000000000000274.
21. Mochizuki T, Tsukamoto E, Kuge Y, Kanegae K, Zhao S, Hikosaka K, et al. FDG uptake and glucose transporter subtype expressions in experimental tumor and inflammation models. J Nucl Med. 2001;42:1551-5.
22. Keijsers RG, van den Heuvel DA, Grutters JC. Imaging the inflammatory activity of sarcoidosis. Eur Respir J. 2013;41:743-51. doi:10.1183/09031936.00088612.
23. Herbst RS, Onn A, Sandler A. Angiogenesis and lung cancer: prognostic and therapeutic implications. Journal of clinical oncology : official journal of the American Society of Clinical Oncology. 2005;23:3243-56. doi:10.1200/JCO.2005.18.853.
24. Folkman J. Angiogenesis in cancer, vascular, rheumatoid and other disease. Nature medicine. 1995;1:27-31.

25. Guillaumond F, Leca J, Olivares O, Lavaut MN, Vidal N, Berthezene P, et al. Strengthened glycolysis under hypoxia supports tumor symbiosis and hexosamine biosynthesis in pancreatic adenocarcinoma. Proc Natl Acad Sci U S A. 2013;110:3919-24. doi:10.1073/pnas.1219555110.
26. Navin N, Kendall J, Troge J, Andrews P, Rodgers L, McIndoo J, et al. Tumour evolution inferred by single-cell sequencing. Nature. 2011;472:90-4. doi:10.1038/nature09807.
27. Hensley CT, Faubert B, Yuan Q, Lev-Cohain N, Jin E, Kim J, et al. Metabolic Heterogeneity in Human Lung Tumors. Cell. 2016;164:681-94. doi:10.1016/j.cell.2015.12.034.
28. Wang L, Zhu B, Zhang M, Wang X. Roles of immune microenvironment heterogeneity in therapy-associated biomarkers in lung cancer. Semin Cell Dev Biol. 2017;64:90-7. doi:10.1016/j.semcdb.2016.09.008.
29. Gould MK, Maclean CC, Kuschner WG, Rydzak CE, Owens DK. Accuracy of positron emission tomography for diagnosis of pulmonary nodules and mass lesions: a meta-analysis. JAMA. 2001;285:914-24. doi:10.1001/jama.285.7.914.
30. Graeber GM, Gupta NC, Murray GF. Positron emission tomographic imaging with fluorodeoxyglucose isefficacious in evaluating malignant pulmonary disease. J Thorac Cardiovasc Surg. 1999;117:719-27. doi:10.1016/S0022-5223(99)70292-8.

Figures

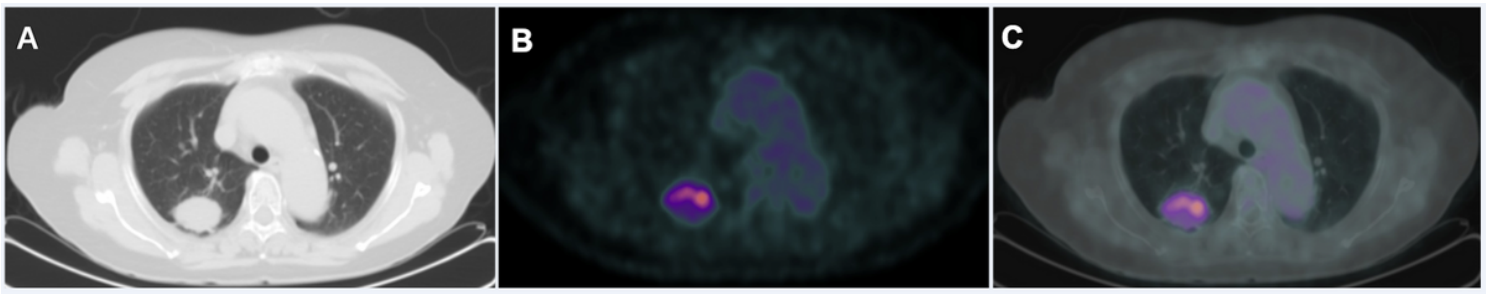

Figure 1

Images from a 65-year-old female patient with adenocarcinoma. Transaxial CT (A) showed a nodule in the right upper lobe. The nodule presented profound FDG uptake with a SUVmax of 6.4 on transaxial PET (B) and MIP (C) images. The FMSD in proximal region of nodule was significantly higher than that of distal region and the score of V-FMSF was 5, indicating malignant lesion.

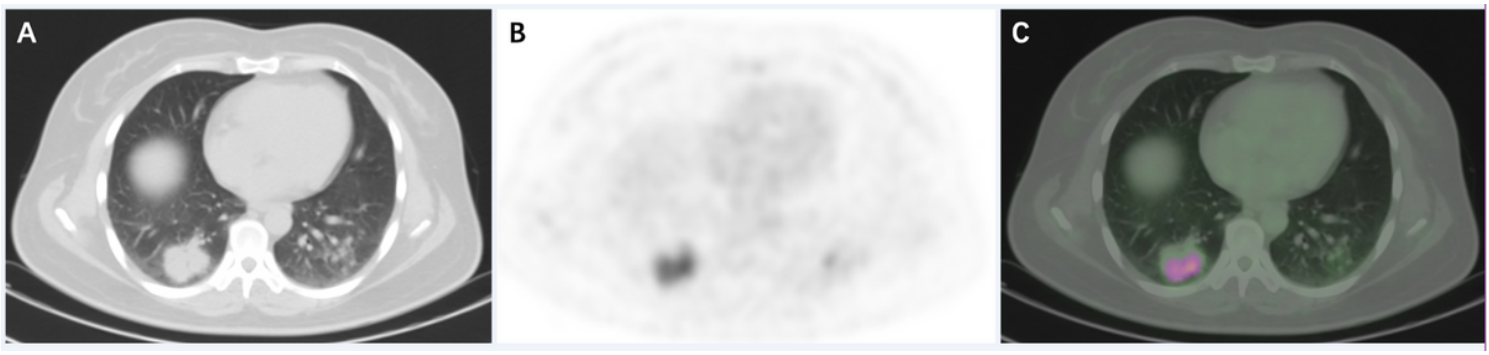

Figure 2

Images from a 49-year-old female patient with tuberculosis. Transaxial CT (A) showed a mass in the right lower lobe. The lesion presented profound FDG uptake with a SUVmax of 8.4 on transaxial PET (B) and MIP (C) images. The FMSD in proximal region of lesion was significantly lower than that of distal region and the score of V-FMSF was 1, indicating benign lesion.

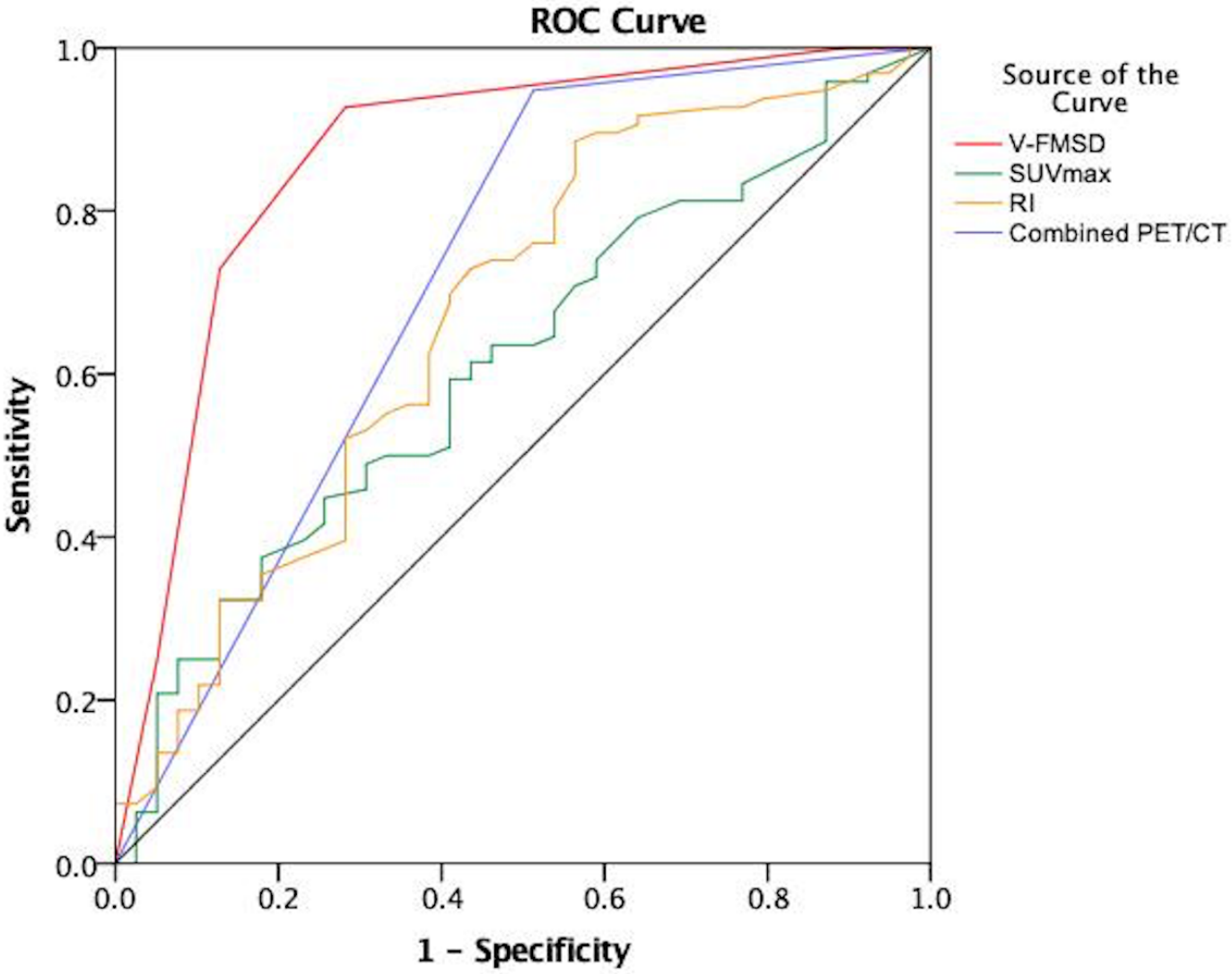

Figure 3

The ROC curves plotted by different diagnostic methods.